Poly(methyl methacrylate) Film Dissolution and Solvent Diffusion Coefficients: Correlations Determined Using Laser Interferometry–Fluorescence Quenching and Pulsed-Gradient Spin-Echo NMR Spectroscopy

X. X. Zhu,† F. Wang, T. Nivaggioli, M. A. Winnik, and P. M. Macdonald*

Department of Chemistry and Erindale College, University of Toronto, Toronto, Ontario, Canada M5S 1A1

Received September 15, 1992; Revised Manuscript Received August 24, 1993•

ABSTRACT: We correlate the results of pulsed-gradient spin-echo (PGSE) nuclear magnetic resonance (NMR) measurements of solvent self-diffusion coefficients in binary poly(methyl methacrylate) (PMMA) mixtures with laser interferometry–fluorescence quenching (LIFQ) measurements of PMMA film dissolution for a series of identical ketone and ester solvents. Within a homologous solvent series, the self-diffusion coefficients as well as film dissolution rates decrease in tandem with increasing solvent molecular size and cross-section. When self-diffusion coefficients are compared, little difference is found between esters and ketones of nomially identical molecular size. However, systematic differences in film dissolution rates are evident when comparing ketone and ester solvents. These differences are eliminated when film dissolution rates for esters and ketones are compared on the basis of the solvent free volume parameters extracted from the PGSE NMR self-diffusion coefficient data using Fujita's free volume theory.

Introduction

The influence of molecular size and shape on diffusion in polymers is an important issue, not only from a fundamental scientific standpoint, but also with regard to technical concerns such as the optimization of materials design and processing. In microelectronic device fabrication, for instance, solvent diffusion during solvent-processing of photoresists leads to swelling at the polymer–solvent interface and can limit the attainable resolution. Diffusion in polymers occurs through molecular jumps into the voids or "free volume" in the polymer matrix, and free volume theories of varying degrees of complexity, including those of Fujita,[1] Cohen and Turnbull,[2,3] and Vrentas and Duda,[4,5] have proved successful in relating diffusion coefficients to critical parameters such as the polymer volume fraction, the free volume contributed by the polymer versus solvent, and the temperature. Parallel developments in methods for measuring diffusion coefficients, such as the pulsed-gradient spin-echo (PGSE) nuclear magnetic resonance (NMR) technique,[6,7] have lead to a profusion of studies of polymer–solvent mixtures including polyisobutylene–benzene,[8] poly(methyl methacrylate)/poly(*n*-butyl methacrylate)–methyl ethyl ketone,[9] polystyrene–tetrahydrofuran,[10] poly(isopropyl acrylate)–chloroform,[1] and polystyrene–toluene,[12] among others (for reviews see von Meerwall[13] and Blum[14]).

Specific studies of the influence of the molecular size and shape of a diffusing species on its diffusion coefficient, in which a homologous series of diffusants is examined within the same polymer matrix, are far less common. Examples include the gravimetric sorption rate measurements by Berens and Hopfenberg of the diffusion of a range of C_1 to C_6 organic vapors at trace concentrations in glassy poly(vinyl chloride) (PVC), polystyrene (PS), and poly(methyl methacrylate) (PMMA).[15] These researchers conclude that an anisometric molecule diffuses through a glassy polymer matrix preferentially along its long molecular axis. Large molecules, such as the series of di-*n*-alkyl phthalate plasticizers in PVC investigated by Storey *et al.*[16] using a mass uptake technique, likewise exhibit anisotropic diffusion through the polymer matrix, and the effects of molecular shape can be accounted for via an extension of the standard free volume theory.[17] Von Meerwall et al.[18] using PGSE NMR demonstrated that, when one separates the effects of molecular weight from those of molecular shape, the diffusion of highly anisometric plasticizer molecules in PVC is clearly anisotropic.

Still fewer in number are studies which combine systematic measurements of diffusion with direct comparison to measurements on a diffusion-dependent process such as polymer film dissolution. In this paper we correlate the results of PGSE NMR measurements of solvent self-diffusion coefficients in binary PMMA mixtures with laser interferometry–fluorescence quenching (LIFQ) measurements of PMMA film dissolution for a series of identical ketone and ester solvents. Such a comparison reveals that, within a homologous solvent series, the self-diffusion coefficients as well as film dissolution rates decrease in tandem with increasing solvent molecular size and cross-section. When solvent self-diffusion coefficients are compared at identical volume fractions in mixtures with PMMA, little difference is found between esters and ketones of nominally identical molecular size. However, systematic differences in PMMA film dissolution rates are evident when comparing the same ketone and ester solvents. These differences are eliminated when film dissolution rates for esters and ketones are compared on the basis of the solvent free volume parameters extracted from the PGSE NMR self-diffusion coefficient data using Fujita's free volume theory.

Experimental Section

Materials. Methyl acetate (MAc), ethyl acetate (EAc), propyl acetate (PAc), isopropyl acetate (iPAc), butyl acetate (BAc), methyl propionate (MPr), methyl butyrate (MBu), and methyl isobutyrate (MiBu) were purchased from Aldrich (Milwaukee, WI). PAc and iPAc were further purified by redistillation prior to use. The other solvents were used without further purification.

Diffusion Coefficient Sample Preparation. The solvent–polymer mixtures for PGSE NMR measurements were prepared

* To whom correspondence should be addressed.
† Current address: Department of Chemistry, University of Montreal, Montreal, Quebec, Canada H3C 3J7.
• Abstract published in *Advance ACS Abstracts*, October 15, 1993.

0024-9297/93/2226-6397$04.00/0

as described previously.[19] Known amounts of PMMA (Aldrich, Milwaukee, WI: M_w = 60 000) plus the respective solvent were transferred into 5-mm NMR sample tubes which were then sealed. The samples were heated overnight above the glass transition temperature of PMMA (105 °C) in an oven preheated to 150–160 °C. Overheating was carefully avoided to prevent decomposition of PMMA. The samples were centrifuged back and forth at least twice to ensure that homogeneous mixing was attained. The selected esters were generally adequate solvents for PMMA and mixed with the polymer, with the exception of BAc. The mixture filled ca. 3 cm in height in the NMR tube.

Pulsed-Gradient Spin-Echo NMR Experiments. An MRI (magnetic resonance imaging) probe with actively shielded gradient coils (Doty Scientific, Columbia, SC) was installed in a Chemagnetics CMX 300 NMR spectrometer operating at 300 MHz for protons. A standard Stejskal-Tanner PGSE sequence ($90°_x$–τ–$180°_y$–τ, with gradient pulses during τ)[6] was used. In this study, the PGSE experiments were performed at 23 °C, and the gradient pulse was applied to the z direction only. It was necessary to use two levels of gradient strength, a lower level (ca. 0.02 T/m) at low polymer concentrations and a higher level (ca. 1.20 T/m) at higher polymer concentrations. The lower gradient strength was calibrated by using the diffusion coefficients of water ($D = 2.34 \times 10^{-9}$ m^2/s) and 2 vol % H_2O in D_2O ($D = 1.9 \times 10^9$ m^2/s)[20,21] (see eq 1 in the following section). In the case of the higher gradient, a sample of 64.2 wt % PMMA in acetone ($D = 5.11 \times 10^{-11}$ m^2/s, which could be measured with both the low and high gradient strengths) was used as the calibration standard. The precision of the measured self-diffusion coefficients of the solvent was very good at low gradient strength, the error being estimated as less than 5%; at higher gradient strength, the error was larger due to the occurrence of eddy currents, but in all cases was less than 15%. Particulars regarding the 90° pulse lengths (19 μs), interpulse delays (10–140 ms), recycle delays (15–30 s), spectral widths (5 kHz), data size (2–4K), line broadening (2–5 Hz), and number of acquisitions (8–16 scans) are those noted in the parentheses, unless otherwise mentioned.

For samples of relatively low polymer concentrations, where the solvent T_2 is long, the PGSE NMR method is easily used to measure the self-diffusion coefficients. For samples of high polymer concentrations, however, both a shorter solvent T_2 and smaller diffusion coefficient require the use of a much higher gradient strength, which in turn can cause severe eddy current effects. The presence of eddy currents can both shift the position of the echo maximum and distort its phase.[22] To overcome this problem, we have developed an empirical compensation function based on a method proposed by Hrovat and Wade,[23] as outlined in a previous paper,[19] the details of which will be described in a separate report. When proper eddy current compensation is applied such that the echo position and phase is correct, Fourier transformation of the echo beginning at its maximum yields the corresponding spectrum.

Film Preparation. Films were prepared on $^1/_{16}$-in.-thick Melles Griot synthetic sapphire disk substrates by spin coating using a Headway Research Model EC 101 photoresist spinner. A solution of 8% by weight PMMA (Elvacite 2401; Dupont, Toronto, Canada; M_w = 425 000, M_n = 149 000, M_w/M_n = 2.95) containing 10% phenanthrene-labeled PMMA in toluene was used. The labeled polymer, PHE–PMMA, was synthesized in this laboratory and characterized according to PHE content (0.7 mol % PHE), weight average molecular weight (M_w = 306 000), number average molecular weight (M_n = 155 000), and polydispersity (M_w/M_n = 2.95). A spinning rated of 2000 rpm for 60 s gave films ca. 0.8 μm thick. The disks were placed on a high-mass aluminum plate, baked for 1 h at 140 °C in a vacuum oven at a pressure of 1 Torr, and allowed to cool slowly to room temperature over a period of 6 h. Moisture was excluded from the films by using an oven equipped with a container of silica gel desiccant and by storing the films in a desiccator prior to dissolution.

Laser Interferometry and Fluorescence Quenching Experiments. The complete experimental setup is described elsewhere.[24] It consists of a flow cell fitted inside the chamber of a SPEX FLUOROLOG II spectrofluorometer and connected to 1-mW diode laser (673.0 nm) via a three-branch randomized fiber-optic cable. The reflected light of the laser is detected by a PIN diode photodetector interfaced to an AT-type personal computer for display and processing. Solvent is introduced via a pump to the bottom of the flow cell and is constrained to laminar flow over the surface of the film. The system monitors simultaneously the reflectance of the laser beam and fluorescence from the PHE groups attached to the polymer chains using λ_{ex} = 295 nm and λ_{em} = 370 nm.

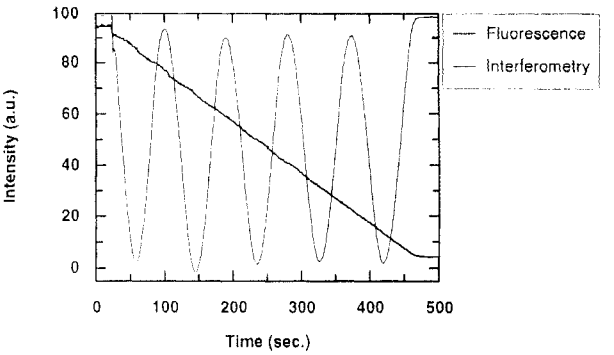

Figure 1. LIFQ results using ethyl acetate as solvent. The PMMA film was prepared by spin coating from a toluene solution (1200 rpm, 30 s) onto a sapphire disk, baked at 120 °C for 1 h under vacuum, and then cooled slowly to room temperature prior to dissolution.

Results and Discussion

Laser Interferometry–Fluorescence Quenching. A typical LIFQ result for dissolution of a PMMA film by the ester solvent EAc is shown in Figure 1. In laser interferometry one observes the interference between light reflected from the polymer–solvent versus the polymer–substrate interface. The change in film thickness over time modulates this interference between constructive and destructive interactions, leading to a sinusoidal variation in reflectivity versus time. In Figure 1 the regular sinusoidal interference pattern is established only after several seconds of delay following the initial sharp decrease in reflectivity when solvent enters the flow cell. This delay represents the time lag necessary for the formation of the initial gel layer (IGL). Once the interference pattern is established, the extrema of the interferogram are equally spaced. As described previously,[25] from the period of the sinusoidal trace one can reconstruct the thickness versus time curve. Such curves are virtually linear, and from their slope one may calculate the dissolution rate (DR).

Superimposed on the interferometry results in Figure 1 is the decay in fluorescence intensity from PHE–PMMA. For ketone solvents this intensity drop is due to quenching of the PHE fluorescence. For the ester solvents, because they are not quenchers of the fluorescence of the PHE groups, the decrease in fluorescence intensity is due instead to the loss of PHE groups as the polymer dissolves and is flushed from the system. Within the noise limit, the fluorescence trace is linear throughout the experiment except at the very beginning and the very end of dissolution. The dissolution rates calculated from the linear portion of the fluorescence decay curves are virtually identical to those obtained from laser interferometry as described above.

Values of DR for the three different ketone and four different ester solvents investigated here are listed in Table I. Most striking is the fact that there is an almost 20-fold decrease in the rates of PMMA film dissolution as the size of the solvent increases from MAc to EAc to PAc. A similar decrease in the rate of PMMA film dissolution with increasing molecular size is observed with the ketone solvents ACT, MEK, and MPK. However, ester solvents always dissolve the PMMA films at faster rates than ketone

Table I. Rates of PMMA Film Dissolution by Ketone and Ester Solvents

solvent	DR[a] (nm/s)	solvent	DR[a] (nm/s)
ACT	6.4(±1.1)	MAc	9.1(±0.8)
MEK	2.6(±0.1)	EAc	3.6(±0.2)
MPK	0.6(±0.05)	MPr	4.6(±0.1)
		PAc	0.5(±0.02)

[a] Average values for five determinations are given while the numbers in parentheses indicate the ranges observed.

solvents of similar molecular size and shape, i.e., MEK vs MAc and MPK vs MPr or EAc.

Pulsed-Gradient Spin-Echo NMR Spectroscopy. For isotropic diffusion in a homogeneous magnetic field, where the residual gradient G_0 is negligible, the amplitude ($A(2\tau)$) of the NMR signal at time 2τ following the application of the PGSE pulse sequence is related to the diffusion coefficient D according to

$$A(2\tau) = A'(0) \exp[-\gamma^2 G^2 D \delta^2 (\Delta - \delta/3)] \quad (1)$$

where G is the pulsed-gradient strength, δ the duration of the gradient, Δ the interval between the gradients, τ the pulse interval, and γ the magnetogyric ratio.[7] The effect of T_2 (spin–spin relaxation time) is constant when τ is kept constant, and the effect of T_2 is contained in the term $A'(0)$. The diffusion coefficient can be derived from the slope of a plot of the logarithm of the signal intensity as a function of $\delta^2(\Delta - \delta/3)$ once the gradient strength G is known. The latter can be obtained by calibration with a sample of known diffusion coefficient, as described in the Experimental Section.

The PMMA proton signals, having a much shorter T_2, do not appear in the spectrum. Our plots of the logarithm of the peak intensities as a function of $\delta^2(\Delta - \delta/3)$ are uniformly linear for all solvents and polymer volume fractions reported here. Certain esters, although desirable from the viewpoint of a complete structural series comparable to the ketone series reported previously,[19] have been omitted. Thus, we do not present data for the ester solvents isobutyl acetate, *tert*-butyl acetate, and methyl trimethylacetate because they do not form homogeneous mixtures with PMMA. For butyl acetate at polymer fractions greater than 0.2, similar mixing problems were encountered, and we refrain from reporting diffusion data for this solvent as well.

Figure 2 illustrates the dependence of the solvent self-diffusion coefficient on the volume fraction of polymer for the individual esters investigated here. In all cases, increasing the PMMA volume fraction causes a progressive decrease in the self-diffusion coefficient of the solvent. In Figure 2A, a series of alkyl acetate esters are compared. It is evident that for the linear acetate esters the self-diffusion coefficients decrease in the order MAc > EAc > PAc, as the length of the ester alkyl group increases from one to three carbons. Increasing the profile or geometric cross-section of the alkyl ester group without altering molecular mass leads to a further reduction of the self-diffusion coefficient such that PAc > iPAc. Similar effects are observed with the methyl esters (Figure 2B): the self-diffusion coefficients of linear methyl esters decrease in the order MAc > MPr > MBu, while branching of the carboxylate group decreases the self-diffusion coefficient such that MBu > MiBu.

Free Volume Parameters. The fitted curves in Figure 2 are generated using Fujita's simple free volume theory.[1] Fujita modified Doolittle's relation between the self-diffusion coefficient and the probability for a molecule to

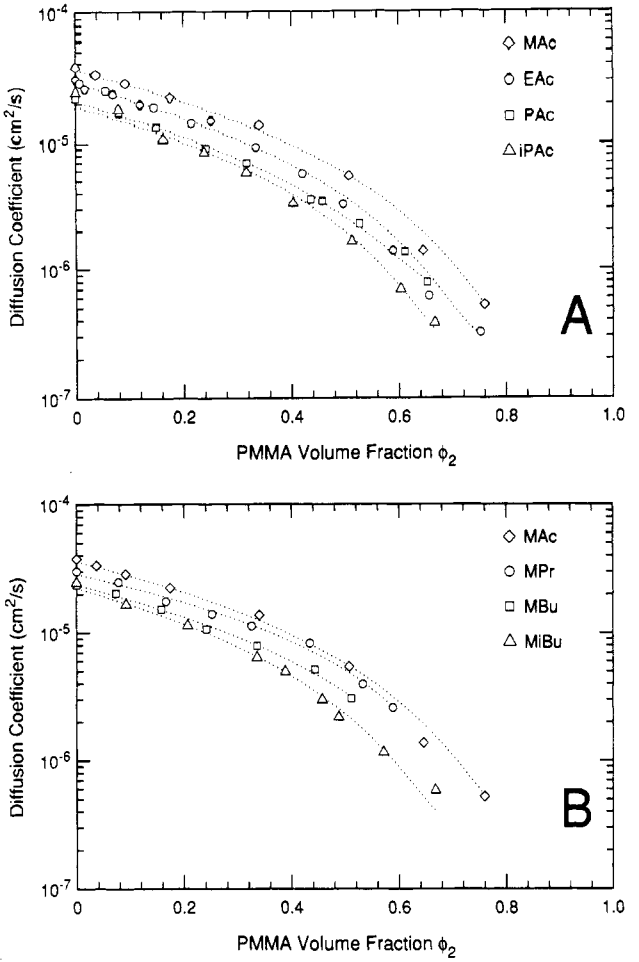

Figure 2. Self-diffusion coefficients of selected ester solvents in PMMA as a function of PMMA volume fraction: (a) various linear and branched alkyl acetates, (B) various linear and branched methyl carboxylates. The experimental data are fitted with Fujita's free volume theory as described in the text.

encounter a void or free volume exceeding a given size and obtained the expression

$$D = RTA \exp(-B/f) \quad (2)$$

where f is the total free volume of the system, B is the minimum hole size or jump size required for the diffusion of a given molecule or molecular segment, A is a factor depending on the size and shape of the diffusing molecule, and R and T are the gas constant and absolute temperature, respectively. The free volume of a mixed system is assumed to equal the sum of the fractional free volumes contributed by the individual components (e.g., solvent and polymer) according to

$$f = f_1\phi_1 + f_2\phi_2 = f_2 + \beta\phi_1 \quad (3)$$

where ϕ_i is the volume fraction of component i with free volume f_i. The subscripts 1 and 2 will always refer to the solvent and the polymer, respectively. Note that $\beta = f_1 - f_2$.

Fujita's free volume theory can be expressed as functions of temperature and polymer concentration relative to a reference state. At identical temperatures, various reference states have been used including pure polymer,[8-11] mixed polymer–solvent,[11] and pure solvent.[9,19] Primarily it is a question of experimental convenience and the reliability of the diffusion data. Since we are concerned with solvent diffusion in polymer mixtures and, moreover, the precision of the PGSE NMR measurements is greatest at low polymer concentrations, it is natural that we choose

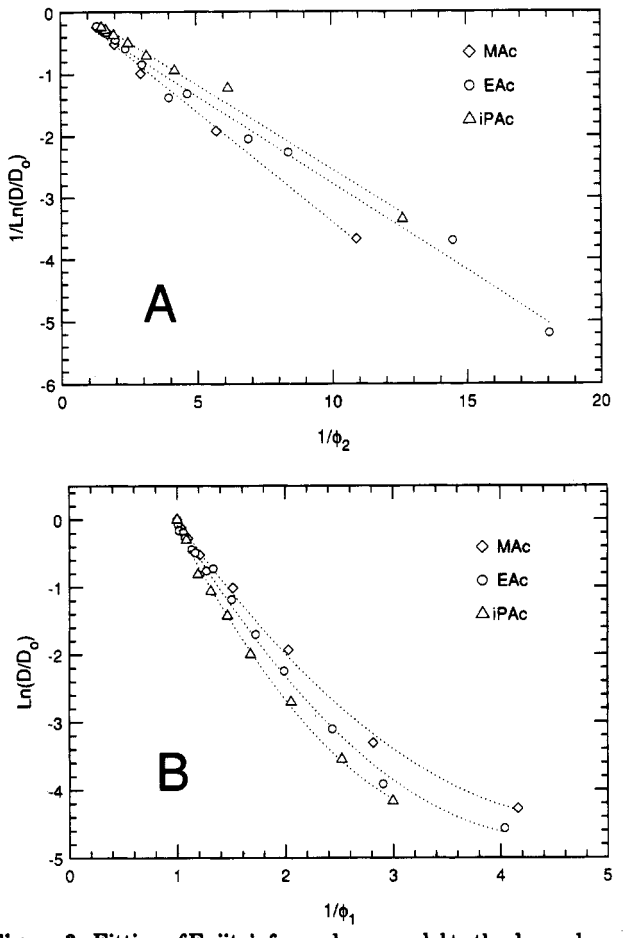

Figure 3. Fitting of Fujita's free volume model to the dependence of solvent self-diffusion coefficients on the volume fraction of PMMA: (A) $[\ln(D/D_o)]^{-1}$ as a function of the inverse volume fraction of PMMA, ϕ_2^{-1}, for selected ester solvents (MAc, EAc, and iPAc), (B) $\ln(D/D_0)$ as a function of the inverse fraction of solvent, ϕ_1^{-1}, for the same selected ester solvents. In all cases the diffusion coefficient of the pure solvent is used as the reference point. For clarity, only representative solvents are shown here.

the pure solvent as the reference state. Assuming B as a constant throughout the concentration range, we have

$$\left[\ln\frac{D}{D_0}\right]^{-1} = \frac{f_1}{B} - \frac{f_1^2}{B\beta}\frac{1}{\phi_2} \tag{4}$$

in which D_0 is the self-diffusion coefficient of the reference state. If free volume theory correctly accounts for the dependence of diffusion on the polymer volume fraction, a plot of $1/\ln(D/D_o)$ versus $1/\phi_2$ should be linear with slope and intercept equal to $-f_1^2/(B\beta)$ and f_1/B, respectively. Figure 3A shows examples of such plots for three representative ester solvents. The fitted lines have values of the linear correlation coefficient, r^2, falling in the range 0.998–0.999, as determined by linear regression analysis. It is clear, therefore, that free volume theory adequately describes the dependence of the solvent diffusion coefficients on the PMMA volume fraction. However, the standard deviations of the intercepts from the fits with eq 4 are quite large. This difficulty arises because the values of the intercepts are extremely sensitive to small deviations in the reference state diffusion coefficient, while the slope is relatively insensitive, as noted previously by others.[1] In contrast, the slopes of the fitted lines (see Table II) are determined with very small standard deviations. The curves in Figure 2 are generated with the slope values in Table II. The correspondence between experiment and the free volume model is excellent.

Table II. Diffusion Coefficients, Viscosities, and Free Volume Parameters of the Esters at 23 °C

	D (10^{-5} cm^2/s)	η^a (cP)	R^b (Å)	$f_1^2/(B\beta)^c$	$B/f_1{}^d$
MAc	3.71	0.372	1.57	0.364	1.986
EAc	3.04	0.437	1.63	0.316	2.232
PAc	2.23	0.565	1.72	0.325	2.509
iPAc	2.41	0.533	1.69	0.266	3.081
MPr	3.01	0.443	1.63	0.425	2.338
MBu	2.36	0.558	1.65	0.470	2.253
MiBu	2.42	0.506	1.77	0.333	2.658

[a] Assembled from literature.[26] [b] Calculated from the Stokes–Einstein equation. [c] $-f_1^2/(B\beta)$ is the slope from eq 4. [d] $-B/f_1$ is the slope from eq 5.

One would like to interpret the free volume parameters in molecular terms, but the most reliable quantity, $f_1^2/(B\beta)$, is somewhat opaque to interpretation. The quantity f_1/B is more directly connected to molecular specifics, but as mentioned above, the value obtained from plots of eq 4 appears somewhat unreliable. Another means of obtaining a value for the free volume parameter f_1/B involves assuming that over some limited range the fractional free volume contributed by the polymer is negligible relative to that of the solvent. Since the solvent self-diffusion coefficients decrease with increasing polymer volume fraction, it must be true that the polymer free volume is much smaller than that of the solvent. At lower polymer concentrations (i.e., $\phi_1 \gg \phi_2$), the contribution of the polymer to the total free volume of the system should be negligible if $f_2 \ll f_1$, and one can simplify eq 4 to obtain

$$\ln\frac{D}{D_0} = \frac{B}{f_1} - \frac{B}{f_1}\frac{1}{\phi_1} \tag{5}$$

Figure 3B illustrates the results of plotting $\ln(D/D_0)$ for representative solvents according to eq 5, where $\ln(D/D_0)$ again refers to the pure solvent as a reference state. Over the full range of polymer concentrations such plots are clearly nonlinear so that, in general, it is inappropriate to assume the free volume contributed by the polymer to be negligible. However, at solvent volume fractions of about 0.80 and greater, such plots are quite nearly linear. The slope of the linear portion equals $-B/f_1$, for the concentration range over which the simplifying assumption is valid, and values for the individual solvents are listed in Table II.

Correlation between Dissolution Rate and Diffusion Coefficient. Both film dissolution rates and self-diffusion coefficients depend on the details of the solvent molecular structure. Figure 4A shows the correlation between the film dissolution rate (DR) and the self-diffusion coefficient of the various ketone and ester solvents at 50 vol % PMMA (D_{50}). Within a homologous series DR and D_{50} are closely linked, with DR decreasing in step with a decreasing D_{50}. However, DR is always greater for a given ester solvent relative to a ketone solvent of comparable D_{50}. Identical behavior is obtained if one correlates DR with the self-diffusion coefficient of the pure solvent D_0, which is in keeping with the observation that the absolute value but not the relative magnitude of the self-diffusion coefficients of the various solvents is affected by mixing with PMMA.

The diffusion coefficients of the pure solvents are listed in Table II. They decrease with increasing molecular weight in strict adherence to a power law of the form

$$D = k(T)M^a \tag{6}$$

where a equals −1. The ketone and ester solvents have nearly identical values of the proportionality constant $k(T)$ in eq 6, indicating the preeminence of molecular size as

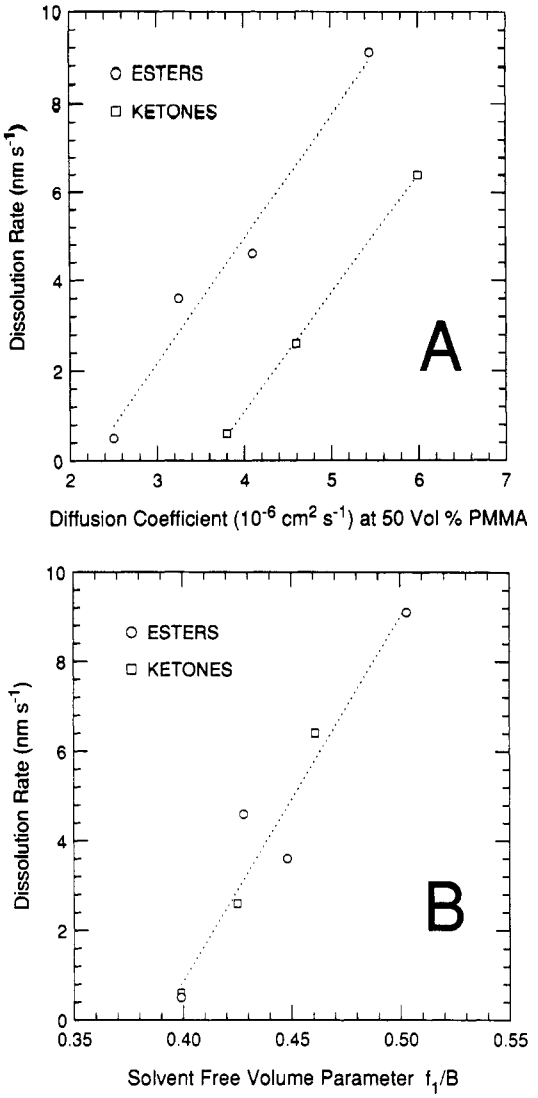

Figure 4. Correlations between the PMMA film dissolution rate (DR) and the solvent self-diffusion coefficient (D) in mixtures with PMMA. (A) DR versus D for various ester and ketone solvents. The self-diffusion coefficients of ketone solvents are those reported previously.[19] Since solvent self-diffusion coefficients become increasingly problematic to measure using PGSE NMR at higher PMMA volume fractions, the values at 50 vol % PMMA represent the highest polymer concentration common to all seven solvents. (B) DR versus f_1/B, the solvent free volume obtained from the slope of eq 5 as shown and listed in Table II.

an affecter of relative rates of diffusion among the pure solvents at constant temperature. Using the Stokes–Einstein equation for spherical particles,

$$D = kT/(6\pi\eta R) \quad (7)$$

one may relate the diffusion coefficient D, measured in a medium of viscosity η, to the effective dynamic radius R, where k and T are the Boltzmann constant and the absolute temperature, respectively. Table II lists the effective dynamic radii calculated using the Stokes–Einstein equation and viscosity data assembled from the literature.[26] If one attempts to correlate the PMMA film dissolution rate with the effective dynamic radius of the diffusing solvent molecule, one again encounters a systematic difference between the ketone and ester solvent series.

The film dissolution rates for the ketones and esters correlate best with the free volume parameter f_1/B, which is a measure of the free volume available for a molecule (or molecular segment) to jump into as it diffuses. Figure 4B shows the quality of this correlation, and it is evident that any differences between ketone and ester solvents have been largely eliminated.

The dissolution of glassy polymer films is conveniently modeled in terms of three distinct steps. First, solvent molecules diffuse via a Fickian process into the rigid polymer matrix. Second, the solvent molecules promote the formation of a solvent-swollen gel layer or transition layer. Finally, the polymer molecules themselves diffuse from the gel layer into the pure solvent. If the initial Fickian diffusion step were rate-limiting, a $t^{1/2}$ time dependence of film dissolution would be anticipated, a situation clearly at odds with the observations. In the case II diffusion model the film thickness is predicted to display a linear dependence on time, and the rate-limiting step is the formation of the gel layer. The LIFQ results on ketone and ester solvent dissolution of PMMA films apparently conform to a case II diffusion model. The correlation of dissolution rates with solvent free volume parameters indicates that both solvent diffusion into and polymer diffusion out of the film may influence rates of film dissolution. In the present case the various ketones and esters investigated are each relatively good solvents for PMMA, although some systematic decrease in the thermodynamic compatibility between polymer and solvent is expected as the solvent molecular size increases.[27] Hence, the rate at which an individual PMMA molecule can disentangle itself from the polymer film depends on the diffusion coefficient of individual polymer segments which depends, in turn, upon the local free volume available for segmental jumps. In the concentration range at which disentanglement occurs the available free volume is determined largely by the free volume of the solvent.

Summary and Conclusions

We have compared rates of PMMA film dissolution, determined using LIFQ, and solvent self-diffusion coefficients in mixtures with PMMA, determined using PGSE NMR, for a series of identical ester and ketone solvents. In general, increasing solvent molecular size decreases both film dissolution rates and self-diffusion coefficients. In particular, however, systematic differences between the dissolution rates due to ketones versus esters of identical molecular size were observed when compared on the basis of the self-diffusion coefficients. The decrease of the solvent self-diffusion coefficients upon increasing the PMMA volume fraction fit a simple free volume theory. When compared on the basis of the free volume parameters extracted from the dependence of the self-diffusion coefficients on the PMMA volume fraction, the film dissolution rates for ketones and esters fell on a common line. This indicates that both solvent diffusing into and polymer exiting from the film can play a determining role in the rate of film dissolution.

Acknowledgment. We acknowledge the financial support for this work in the form of an NSERC Strategic Grant from the Natural Sciences and Engineering Research Council of Canada.

References and Notes

(1) Fujita, H. *Adv. Polym. Sci.* **1961**, *3*, 1.
(2) Cohen, D. C.; Turnbull, D. *J. Chem. Phys.* **1959**, *31*, 1164.
(3) Turnbull, D.; Cohen, D. C. *J. Chem. Phys.* **1961**, *34*, 120; **1970**, *52*, 3038.
(4) Vrentas, J. S.; Duda, J. L.; Ling, H. C. *J. Polym. Sci., Polym. Phys. Ed.* **1985**, *23*, 275.
(5) Vrentas, J. S.; Duda, J. L.; Ling, H. C.; Hou, A. C. *J. Polym. Sci., Polym. Phys. Ed.* **1985**, *23*, 289.
(6) Stejskal, E. O.; Tanner, J. E. *J. Chem. Phys.* **1965**, *42*, 288.

(7) Stilbs, P. *Prog. NMR Spectrosc.* **1987**, *19*, 1.
(8) Boss, B. D.; Stejskal, E. O.; Ferry, J. D. *J. Phys. Chem.* **1967**, *71*, 1501.
(9) Hwang, D. H.; Cohen, C. *Macromolecules* **1984**, *17*, 1679; **1984**, *17*, 2890.
(10) von Meerwall, E. D.; Amis, E. J.; Ferry, J. D. *Macromolecules* **1985**, *18*, 260.
(11) Blum, F. D.; Nurairaj, B.; Padmanabhan, A. S. *J. Polymn. Sci., Polym. Phys. Ed.* **1986**, *24*, 493.
(12) Pickup, S.; Blum, F. D. *Macromolecules* **1989**, *22*, 3961.
(13) von Meerwall, E. D. *Adv. Polym. Sci.* **1983**, *54*, 1.
(14) Blum, F. D. *Spectroscopy* **1986**, *1*, 32.
(15) Berens, A. R.; Hopfenberg, H. B. *J. Membr. Sci.* **1982**, *10*, 283.
(16) Storey, R. B.; Mauritz, K. A.; Cox, B. D. *Macromolecules* **1989**, *22*, 289.
(17) Mauritz, K. A.; Storey, R. B.; George, S. E. *Macromolecules* **1990**, *23*, 441.
(18) von Meerwall, E. D.; Skowronski, D.; Hariharan, A. *Macromolecules* **1991**, *24*, 2441.
(19) Zhu, X. X.; Macdonald, P. M. *Macromolecules* **1992**, *25*, 4345.
(20) Mills, R. *J. Phys. Chem.* **1973**, *77*, 685.
(21) James, T. L.; McDonald, G. G. *J. Magn. Reson.* **1973**, *11*, 58.
(22) van Vaals, J. J.; Bergman, A. H. *J. Magn. Reson.* **1990**, *90*, 52.
(23) Hrovat, M. I.; Wade, C. G. *J. Magn. Reson.* **1981**, *44*, 62; **1981**, *45*, 67.
(24) Nivaggioli, T.; Dimnik, G. P.; Wang, F.; Winnik, M. A.; Smith, B. A. *Appl. Opt.* **1992**, *31*, 5956.
(25) Nivaggioli, T.; Wang, F.; Winnik, M. A. *J. Phys. Chem.* **1992**, *96*, 7462.
(26) Viswanath, D. S.; Natarajan, G. *Data Book on the Viscosity of Liquids*; Hemisphere Publishing Corp.: New York, 1989.
(27) Barton, A. F. M. *CRC Handbook of Solubility Parameters and Other Cohesive Parameters*; CRC Press, Inc.: Boca Raton, FL, 1983; p 387.